

See discussions, stats, and author profiles for this publication at: <https://www.researchgate.net/publication/318995078>

A Respiration-Derived Posture Method Based on Dual-Channel Respiration Impedance Signals

Article in IEEE Access · August 2017

DOI: 10.1109/ACCESS.2017.2737461

CITATIONS
10

READS
182

6 authors, including:



Guan-Zheng Liu
Sun Yat-sen University
70 PUBLICATIONS 1,493 CITATIONS

[SEE PROFILE](#)



Wenhui Chen
University of Science and Technology Beijing
9 PUBLICATIONS 134 CITATIONS

[SEE PROFILE](#)

Received July 4, 2017, accepted July 31, 2017, date of publication August 8, 2017, date of current version September 19, 2017.

Digital Object Identifier 10.1109/ACCESS.2017.2737461

A Respiration-Derived Posture Method Based on Dual-Channel Respiration Impedance Signals

**GUANZHENG LIU, KUNYANG LI, LIANRONG ZHENG, WEN-HUI CHEN,
GUANGMIN ZHOU, AND QING JIANG**

Biomedical Engineering, School of Engineering, Sun Yat-sen University, Guangzhou 510275, China

Key Laboratory of Sensing Technology and Biomedical Instrument of Guangdong Province, Guangzhou 510275, China

Guangdong Provincial Engineering and Technology Centre of Advanced and Portable Medical Device, Guangzhou 510275, China

Corresponding author: Qing Jiang (jqing@mail.sysu.edu.cn)

This work was supported in part by the Natural Science Foundation of China under Grant 61401521, in part by the Science and Technology Program of Guangzhou under Grant 2017A01010103, and in part by the Natural Science Foundation of Guangdong province under Grant 2014A030310163.

ABSTRACT Sleep posture has been used as a sleep assessment indicator in home health monitoring and clinical monitoring in recent years. Considering comfort and usability, unobtrusive sleep posture detection is needed. In this paper, we proposed a novel sleep respiration-derived posture (RDP) method based on left and right lung respiration impedance signals. We developed a dual-channel respiratory impedance acquisition system with wireless transmission. Then, support vector machine using radial basis function kernel was applied to recognize four typical sleep postures. Moreover, the performance of the SVM classifier was improved by using backward elimination. *In-situ* experiments with 16 subjects indicated that the RDP method reached an accuracy of 99.67%. Thus, our method is reliable in sleep posture recognition. Furthermore, a whole-night monitoring system based on respiration impedance can be conducted for sleep quality assessment.

INDEX TERMS Respiration derived posture (RDP), respiratory impedance, backward elimination (BE), support vector machine (SVM), radial basis function (RBF).

I. INTRODUCTION

Sleep posture belongs to the important indicators in sleep quality assessment [1]. It is important for the early prevention of some diseases, e.g. pressure ulcers [2] and sleep apnea [3]. Therefore, sleep posture real-time monitoring is advantageous for sleep monitoring at home and hospitals.

To date, researchers have proposed many different ways to automatically monitor sleep postures, including video cameras, accelerometer sensors, pressure sensors and electrocardiogram-derived postures (EDP), highlights of these methods are listed in Table 1. Among them, the video-camera, often regarded as the golden standard, has been used previously to identify sleep postures [4]. However, video recording may have a risk of the invasion of privacy to the users.

Owing to the problem of the camera, many studies have focused on a wearable sleep posture monitoring method by using accelerometers. Borazio et al. used a wrist-worn sensor that recorded three-dimensional acceleration for posture clustering, obtaining an average accuracy of 94% [5].

Wrzus et al. detected sleep postures using acceleration sensors on the sternum and right thigh, which achieved accuracy of 99.7% [6].

As an option, some studies focused on a non-contact sleep posture sensing method with different pressure sensors. Hsia et al. designed a mattress pad with a force-sensing resistor (FSR) to monitor the change of body postures, obtaining an accuracy of 81.43% [7]. Liu et al. designed a dense pressure-sensitive bed sheet system to monitor sleep postures, which only exhibited an accuracy of 83.0% [8]. To improve the accuracy, Yousefi et al. developed a pressure-mapping system with 2048 sensors for sleep posture recognition, which achieved an average accuracy of 97.7% [9]. Though the non-contact sensing method didn't cause discomfort and privacy offence, it was more complex and expensive due to the large number of sensors and the generated high dimensional data.

As an indirect, unloaded and low-cost method, the electrocardiogram (ECG) derived sleep postures method has attracted scientists' attention. This method does not depend

TABLE 1. Comparison with the relation works.

Method	Measurement	Highlight
Direct method	Video camera [4]	Analyzing image sequence of a real time system to evaluate subjects' posture change (gold standard)
	Accelerometer sensor [5]-[6]	Using wearable accelerometer sensors for posture detection with high accuracy (wearable sensor)
	Pressure sensor [7]-[9]	Using multiple pressure sensors for body posture changes (non-contact sensor)
In-direct method	EDP method [10]-[13]	Deriving postures from ECG signal (wearable sensor)
	Our method	Deriving postures from respiration impedance (wearable sensor)

on any sensors and is an alternative approach to monitor sleep posture. The QRS complex of the ECG can be used to estimate body postures [10], [11]. Shen et al. proposed a body position detection method based on fusing multiple heterogeneous features of three-lead surface ECG with a low accuracy of only 66.67% [12]. Lee et al. used the unconstrained morphology of the QRS wave of ECG signals of twelve capacitive coupled electrodes and a conductive textile sheet to estimate body postures, obtaining an accuracy of 98.4% [13]. This method inspired us to develop a sleep RDP method for sleep assessment. Furthermore, we have analyzed the relationship of sleep posture and respiration impedance in our previous work [14]. A high correlation between sleep posture and left and right lung respiration impedance was found. Thus, we hypothesized that there was a potential assessing sleep posture method via left and right lung respiration impedance signals. Based on this hypothesis, we proposed a new indirect sleep posture extraction method based on dual-channel respiratory signals, including the left lung (LL) and right lung (RL) respiratory impedance signals. The main achievements of this work included:

- 1) We presented a novel and effective sleep respiration-derived posture method based on left and right lung respiratory signals. Compared with EDP method, more innovative and effective features were achieved.
- 2) We built and validated a respiratory and sleep posture monitoring system (Fig.1). Our previous study had proved that the dual-channel respiratory impedance system can overcome the effect of the change in sleep posture. Compare with the previous study, the mean absolute error decreased about 25% [14].
- 3) We identified four different sleep postures using three typical classifiers with linear and non-linear features. Using the backward elimination feature selection algorithm, the performance of the classifiers can be improved. Through the 10-fold cross validation, the SVM using RBF kernel is better than the other classifiers.

The rest of this article is organized as follows: Section II introduced our dual-channel impedance plethysmography (IP) system and posture analysis method; In section III, we described our experiment protocol; Section IV presented the results of sleep posture estimation and section V provided a detail discussion of features and classifiers; The conclusion of this paper is summarized in section VI.

II. SYSTEM AND METHOD

A. SYSTEM INTEGRATION

We set up a dual-channel impedance acquisition system to derive postures from respiration signals. The system consisted of three modules: a data processing module in form of a PC, a data acquisition module, impedance test platform and a Zigbee wireless transmission module in form of a USB, as shown in Fig.1-(d).

Data Acquisition Module: The data acquisition modules consisted of an impedance instrument and a multi-channel adapter [15], as shown in Fig.1-(a) and 1-(c).

Impedance Instrument: CC2530 was used with RF wireless transceiver and 14-bit high accuracy A/D converter, which was regarded as the core of the impedance instrument. And the impedance data of respiratory was converted by this part. The impedance instrument provided the exciting current with the body, which had frequency of 50 kHz and amplitude of 1mA.

Multi-Channel Adapter: the multi-channel adapter consisted of the excitation channel and measurement channel [15]. The excitation channel was formed with DDS, VCCS and some peripheral components, which could directly generate sine wave current with adjustable frequency and safety constant amplitude. The measurement channel was formed with phase sensitive demodulation circuit, a 14-bit high accuracy A/D converter circuit and amplifier circuits, which could measure the developing voltage due to applied current. Two-channel impedance signals were simultaneously collected by using the self-designed multi-channel adapter shown in Fig.1-(c).

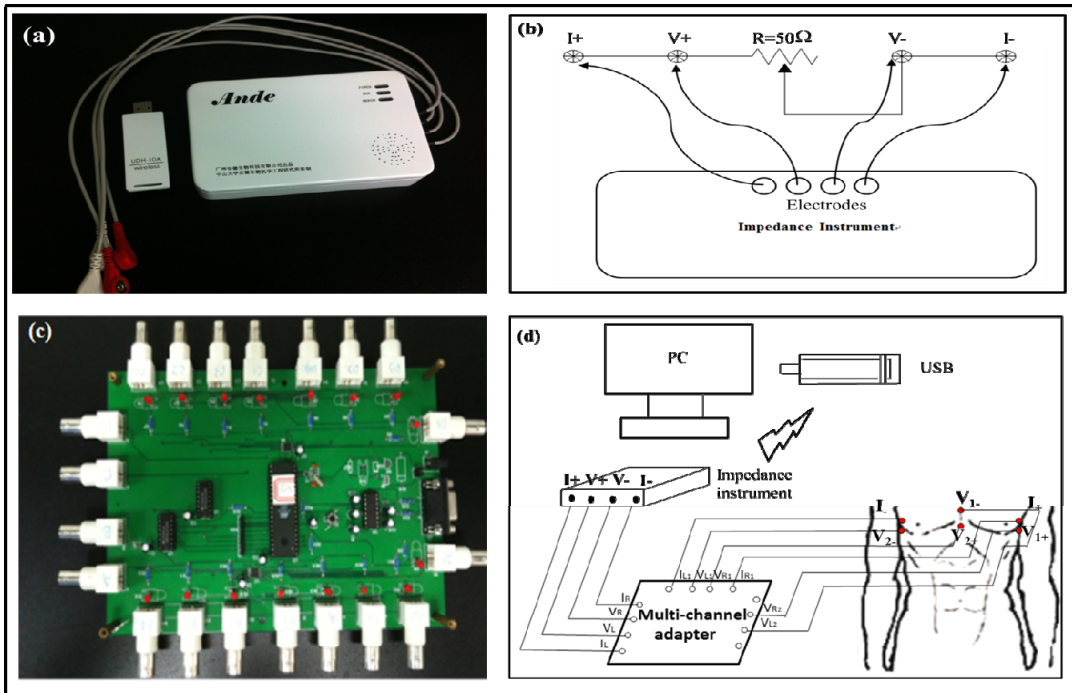


FIGURE 1. The experimental system platform: (a) the impedance instrument and USB transmission module; (b) the impedance test platform of the impedance instrument; (c) the multi-channel adapter module; (d) the schematic diagram of the experimental system platform, and the detail explain of each electrode is given in Table 2.

Zigbee Wireless Transmission Module: It was data receiving module in form of a USB and inserted into the PC [15]. The impedance data was transmitted to PC and figure out in PC.

Impedance Test Platform: To verify the instrument accuracy, we built an impedance test platform [15] (as shown in Fig.1-(b)), which achieved an accuracy of 99.0%.

The safety and effectiveness of the impedance instrument were verified in our previous study. We received the inspection report of China Food and Drug Administration in Guangzhou Medical Equipment Quality Supervision and Inspection Center. The impedance instrument was used to monitor bladder volume [16]. Then, we have finished clinical trials of this study, and received the clinical test summary report of Guangdong Provincial Hospital of Chinese Medicine and the fifth affiliated hospital of Sun Yat-Sen University, Guangzhou, China.

B. SLEEP RESPIRATION-DERIVED POSTURE METHOD

Fig.2 showed the flow diagram of the RDP method. It included four steps: the left and right lung respiration impedance signals were collected by using multi-channel impedance instrument; the respiration volume signals were derived from dual-channel respiration impedance signals; twelve features were derived from dual-channel respiration impedance signals and dual-channel respiration volume signals; sleep posture recognition and validation, including determination of feature subset based on backward elimination algorithm, classifier selection and 10-fold cross validation, as shown in Fig.2.

The left and right lung respiration impedance signals were collected.

The left and right lung respiration volume signals were derived from respiration impedance signals by using pass-band IIR butterworth filter.

Feature extraction

Six features were derived from respiration impedance signals	Six features were derived from respiration volume signals
--	---

Sleep posture recognition

Determine features subset based on backward elimination algorithm	Classifier choose: the performance was compared among SVM, ANN and LDA.
---	---

10-fold cross Validation

FIGURE 2. The flow diagram of RDP method. SVM: support vector machine, ANN: Artificial Neural Network, LDA: Linear Discriminant Analysis.

1) THE LEFT AND RIGHT LUNG RESPIRATION IMPEDANCE SIGNALS

The left and right lung respiration impedance signals were collected by using multi-channel impedance instrument, shown in Fig.1. The sampling frequency of the impedance instrument was set at 6Hz.

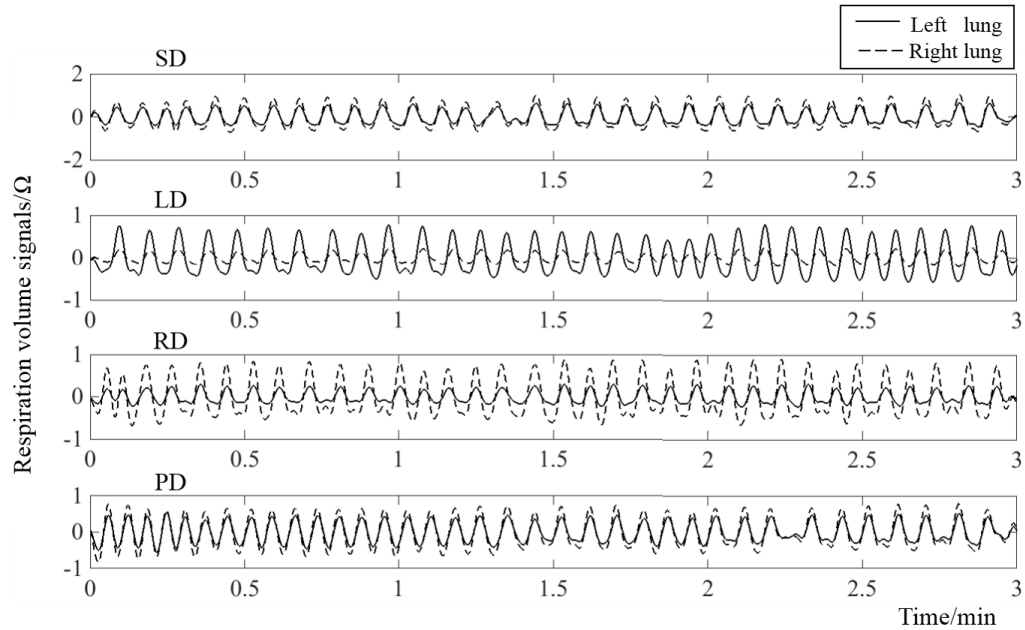


FIGURE 3. Respiratory volume signals of left lung and right lung in the prone decubitus (PD), supine decubitus (SD), left lateral decubitus (LD) and right lateral decubitus (RD).

2) THE LEFT AND RIGHT LUNG RESPIRATION VOLUME SIGNALS

The left and right lung respiration volume signals were derived from dual-channel respiration impedance signals by using a sixth-order IIR Butterworth pass-band filter, which was used to remove the baseline (base impedance value) and measurement noise. The band-pass IIR Butterworth filter has a cutoff frequency between 0.05 and 0.45 Hz. The respiration volume signals were shown in Fig.3.

3) FEATURE EXTRACTION

In this paper, twelve features were extracted from left/right lung impedance signals and LL and RL respiration volume signals, they were as follows:

Respiration Impedance Signals' Features: Six features were used to describe respiration impedance signals of left lung and right lung and they can be divided into two classes. The first-class features were about average level of RL and LL signals including: The difference between the mean impedance of LL and RL respiration impedance signals (M1); the sum of the mean impedance of LL and RL respiration impedance signals (M2); the ratio of the mean impedance of LL and RL respiration impedance signals (M3). The second-class features were about complexity degree of RL and LL signals represented by fuzzy entropy [17]. This aspect included: the difference between the fuzzy entropy of LL and RL respiration impedance signals (F1); the sum of the fuzzy entropy of LL and RL respiration impedance signals (F2); the ratio of the fuzzy entropies of LL and RL respiration impedance signals(F3). The fuzzy entropy represented the complex degree of information.

Respiration Volume Signals' Features: The derived respiration volume signals were analyzed by difference of LL and

RL signals in volume and amplitude. Thus, six features were extracted: the difference between the volume of LL and RL respiration volume signals (V1); the sum of the volume of LL and RL respiration volume signals (V2); the ratio of the volume of LL and RL respiration volume signals (V3); the difference between the amplitude of LL and RL respiration volume signals (A1); the sum of the amplitude of LL and RL respiration volume signals (A2); the ratio of the amplitude of LL and RL respiration volume signals (A3).

4) FEATURE SELECTION WITH BACKWARD ELIMINATION ALGORITHM

The main purpose of feature selection was to determine the feature subset giving the highest discrimination among groups among multiple features, since using all features in one classifier did not achieve the best performance in many cases [18]. In this study, the backward elimination algorithm was used as a feature-optimized approach for the classifiers. Backward elimination algorithm began with all features and iteratively removed one by one [19], [20], which was regarded to be more successful for finding the optimal feature subset [21]. In this article the implementation of the backward elimination method was as follows:

Firstly, feature matrix X are defined as

$$X = [x_1, x_2, \dots, x_n] = \begin{bmatrix} x_1(1) & x_2(1) & \cdots & x_n(1) \\ x_1(2) & x_2(2) & \cdots & x_n(2) \\ \vdots & \vdots & \ddots & \vdots \\ x_1(N) & x_2(N) & \cdots & x_n(N) \end{bmatrix} \quad (1)$$

Where there are one sample's features in each column and each row represents a feature.

TABLE 2. The specific location of electrode configurations.

Position	Electrode Configurations		Physical Positions
	Exciting current	Measuring voltage	
Left Lung	I_+	V_{1+}	I_+ The upper side near the intersection of the horizontal line formed by nipples and the left mid-axillary line. I_- The upper side near the intersection of the horizontal line formed by nipples and the right mid-axillary line.
		V_{1-}	V_{1+} The lower side near the intersection of the horizontal line formed by nipples and the left mid-axillary line. V_{1-} The upper side near the intersection of the horizontal line formed by nipples and the sternal midline.
Right Lung	I_-	V_{2+}	V_{2+} The lower side near the intersection of the horizontal line formed by nipples and the sternal midline. V_{2-} The lower side near the intersection of the horizontal line formed by nipples and the right mid-axillary line.
		V_{2-}	

In our processing, feature subset evaluation criterion was classification ability. Step1, assume there are N features $\{F_i, i = 1, 2, \dots, N\}$. Step2 input all features into classifier to evaluate classification power of $\{F_i, i = 1, 2, \dots, N\}$ and its $N-1$ subset. Each subset has $N-1$ features from $\{F_i, i = 1, 2, \dots, N\}$. Step3, reserve this subset and repeat all these steps if the discrimination ability of one of these subsets is stronger than that of all the other subset and $\{F_i, i = 1, 2, \dots, N\}$; or stop this process and $\{F_i, i = 1, 2, \dots, N\}$ is the optimal feature subset with highest ability in classification.

5) CLASSIFIER EVALUATION

Different classifiers are used in this study, and they are listed as follows:

OVO-SVMs Using Linear, Polynomial, and RBF Kernel: SVM algorithm is originally designed for binary classification problem. When dealing with multi-class problem, it is necessary to construct a suitable multi-class classifier, and OVO-SVMs is one solution. In this paper, we adopted the OVO-SVMsthat was integrated in the libsvm toolbox [22]. SVM is a common machine learning algorithm that has unique advantages in solving the small sample pattern recognition problems because of its excellent generalization ability [23]. For non-linear problem,by mapping the space of input data into a high-dimensional feature space through kernel function, the data points become linear separable or more linear separable in the high-dimensional space [24]. In general, kernel function including three types:linear, polynomial and RBF kernel functions.The RBF kernel function can map the input data into infinite dimension space.

Artificial Neural Network Classifier (ANN): The ANN enables to perform non-linear modeling and adaption, it does not require assumption of any functional relationship between feature and posture in advance. We can adapt the ANN by simply exposing it to new data.

Linear Discriminant Analysis(LDA): LDA, also called fisher linear discriminant, is a classical algorithm of the

pattern recognition. The objective is to find a projection A that maximizes the ratio of between-class scatter against within-class scatter (Fisher's criterion).

III. EXPERIMENT

A. SUBJECTS

16 healthy male subjects from our laboratory participated in the experiment, and were in the age range from 20 to 26 years old. For the subjects, there were no clinically significant signs of respiratory disorders, such as coughing, polypnea, bronchitis, asthma or other lung diseases. The experimental content and processes were carefully explained to the subjects before the experiment by words and pictures. The subjects did not receive any benefits from this study. The experimental protocol was approved by the ethics committee of Guangdong Provincial Hospital of Chinese Medicine.

B. ELECTRODE PLACEMENT

In this study, we measured the tetrapolar impedance, using four electrodes: one pair of electrodes (I_+, I_-) for injecting the excitation current and the other pair (V_+, V_-) for measuring the voltage induced by the current [24]–[27].

The setup of the electrode configurations tested in this paper is shown in Fig.1-(d). The exact physical positions of different electrode configurations are shown in TABLE 2.

C. MEASUREMENT PROCEDURE

Firstly, all the electrodes were affixed to the subjects' bodies, as shown in Fig.1-(d), and then the subjects were instructed to lie in bed.

One cycle included four body postures in the following order: supine decubitus (SD), left lateral decubitus (LD), right lateral decubitus (RD) and prone decubitus (PD) [as shown in Fig.4]. This sequence was the same for each subject. Each posture was held for 3 minutes, before a supervisor verbally instructed the subject to move to the next posture. The subjects were allowed to have small movement during the course of the experiment. The subject was allowed to change posture

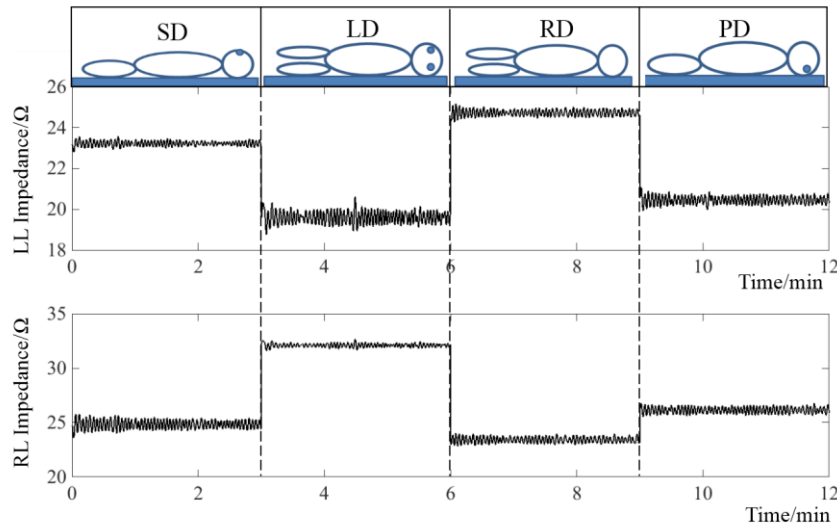


FIGURE 4. Raw data for 12min of controlled posture studies including supine decubitus (SD, 0-3min), left lateral decubitus (LD, 3-6min), right lateral decubitus (RD, 6-9min) and prone decubitus (PD, 9-12min). The respiratory impedance of left lung and right lung were measured by the impedance.

and find a comfortable position within 30–60s, during the period the impedance instrument in shut down and no signal was collected.

After the subject keep stable, another posture was held for another 3 minutes. After finishing one cycle, the second cycle was conducted with the same order of postures as the first cycle for reproducibility.

Data division: All recorded data of each volunteer was divided into eight sections and each section contained. The data of each section was divided into 12 segments, each resulting segment of 15 seconds was defined as a sample to provide a fast recognition [12]. The data of one volunteer was divided into 96 samples, including four different sleep postures (two cycles each).

D. VALIDATION

Statistical analyses were performed between real postures and the outputs of our algorithm. To validate the results obtained from each of the previous analysis, a statistical study was conducted to verify if significant difference was present among the different groups. The results were expressed as mean \pm SD, and all data were analyzed using the statistical software SPSS 14.0(SPSS Inc., Chicago, IL, USA). A p values less than 0.05 was considered significant for all tests.

During the classification phase, a 10-fold cross validation method is applied to check the performance of the classifiers [13]. The whole set of samples is randomly divided into 10 approximately equal and balanced subsets. Then, each time one of these subsets is excluded from the whole set of samples and was set as the test set, and the training set was composed of the remaining subsets. The 10-fold cross validation accuracy is the percentage of correctly classified data. These steps were conducted by MATLAB (version R2009b, The Math Works, Inc., Natick, MA, USA).

IV. RESULTS

In this study, a respiratory impedance acquisition system was developed, and its performance was evaluated in a preliminary study including four sleep postures. The dual-channel (left and right lung) respiratory impedance approach in combination with the SVM classifier obtained an accuracy of 99.67% in sleep posture recognition.

A. FEATURES ANALYSIS

The significant differences among six respiration impedance signals' features and six respiratory volume signals' features of four sleep positions (PD, SD, LD and RD) are shown in Table 3. All the features showed the significant differences among PD, SD, LD and RD except M2. As for M1, M3, F1, F2, F3, V1, V2, V3 and A3, there were significant differences in all pairwise comparisons among PD, SD, LD and RD respectively ($P < 0.05$). As for A1 and A2, there were significant differences in some pairwise comparisons among PD, SD, LD and RD.

B. FEATURE SELECTION AND CLASSIFIER PERFORMANCE

The proposed feature selecting algorithm is applied to select the most compact feature subset from the 12 available features with 3 classifiers.

In total, 1536 samples were obtained. As mentioned before, we adopted a 10-fold cross validation method to check the performance of the classifiers. Table 4 presents the comparison of the classifier's performance and the parameter setting. Through the feature selection algorithm, the irrelevant and redundant features were removed, and the classification accuracy of each classifier had been improved. Specifically, the BE algorithm could significantly improve the performance of the OVO-SVMs using RBF kernel, the final feature subset was composed of only 3 features (TABLE 5),

TABLE 3. The significant difference among PD, SD, LD and RD.

Sleep position	M1 (Ω)	M2 (Ω)	M3 (n.u)	F1 (n.u)	F2 (n.u)	F3 (n.u)
PD	-0.23 \pm 3.09 ^{bcd}	47.72 \pm 10.27	50.09 \pm 3.65 ^{bcd}	-0.02 \pm 0.04 ^{bcd}	0.37 \pm 0.16 ^{bcd}	46.65 \pm 4.98 ^{bcd}
SD	1.41 \pm 2.50 ^{acd}	48.23 \pm 10.85	51.46 \pm 2.66 ^{acd}	-0.04 \pm 0.04 ^{acd}	0.35 \pm 0.14 ^{acd}	42.40 \pm 6.67 ^{acd}
LD	-6.28 \pm 4.27 ^{abd}	48.65 \pm 12.12	43.48 \pm 4.26 ^{abd}	0.06 \pm 0.06 ^{abd}	0.31 \pm 0.13 ^{abd}	60.87 \pm 9.79 ^{abd}
RD	6.71 \pm 4.70 ^{abc}	48.44 \pm 12.09	57.73 \pm 7.27 ^{abc}	-0.08 \pm 0.07 ^{abc}	0.29 \pm 0.13 ^{abc}	35.64 \pm 11.32 ^{abc}
Sleep position	V1 (Ω)	V2 (Ω)	V3 (n.u)	A1 (Ω)	A2 (Ω)	A3 (n.u)
PD	-6.23 \pm 11.21 ^{bcd}	34.78 \pm 12.34 ^{bcd}	45.90 \pm 6.32 ^{bcd}	-0.40 \pm 1.37 ^{bcd}	4.90 \pm 3.26 ^{bcd}	46.13 \pm 11.75 ^{bcd}
SD	-11.81 \pm 10.62 ^{acd}	28.23 \pm 10.96 ^{acd}	40.87 \pm 7.78 ^{acd}	-0.62 \pm 1.08 ^{ad}	4.15 \pm 2.64 ^{acd}	41.69 \pm 11.52 ^{acd}
LD	13.19 \pm 15.96 ^{abd}	37.35 \pm 14.76 ^{abd}	61.95 \pm 11.42 ^{abd}	0.81 \pm 1.30 ^a	3.89 \pm 2.65 ^{ab}	61.64 \pm 13.65 ^{abd}
RD	-18.04 \pm 15.06 ^{abc}	17.76 \pm 8.44 ^{abc}	33.75 \pm 12.57 ^{abc}	-1.27 \pm 1.58 ^{ab}	3.72 \pm 2.71 ^{ab}	34.16 \pm 15.86 ^{abc}

Data are presented as mean \pm SD; For value of features comparison between sleep positions, ^aP<0.05 versus PD, ^bP<0.05 versus SD, ^cP<0.05 versus LD, ^dP<0.05 versus RD. n.u: dimensionless unit.

TABLE 4. Comparison of classifier performance.

Classifier	Parameter	Accuracy(After BE)				
		PD (%)	SD (%)	LD (%)	RD (%)	Total (%)
ANN	12input-1 hidden layer-4 output	65.63	68.23	85.68	79.17	74.69
LDA	N/A	75.78	63.54	86.20	88.54	76.43
SVM	Linear	c=1	79.95	70.83	86.72	90.63
	Polynomial	c=1,d=3, $\gamma = 1/4, r=0$	81.77	55.99	95.57	89.06
	RBF	c=1, $\gamma = 1/4$	100	100	98.70	100
						99.67

and we obtained a total accuracy of 99.67%. The recognition accuracies of PD, SD, LD and RD were 100%, 100%, 98.70% and 100%, respectively. In each postures, SVM using RBF kernel could obtain the highest accuracy in this dataset. Fig.5 illustrates the performance of all classifiers, it can be observed that the performance of the OVO-SVMs using RBF kernel is obviously better than the other classifiers in this dataset, therefore, we choose the OVO-SVMs as the final classifier in this work.

C. OVO-SVMs CLASSIFIER USING RBF KERNEL FOR RDP BASED SLEEP POSTURE RECOGNITION

The confusion matrix of the SVM classifier was shown in Fig.6, the numbers located in the diagonal represent the correct prediction of each posture. Only in the LD posture, 5 segments were incorrectly classified as the SD, the incorrect classified segments didn't significantly affect the result based on our method and the total accuracy was 99.67%. Therefore, we conclude that the proposed RDP method is reliable and can be adapted to monitor sleep posture during sleep.

TABLE 5. Feature selected by the BE algorithm.

Classifier	Feature
ANN	M1, M2, M3, V1, V2, A1, A2, A3, F1, F2, F3
LDA	M1, M2, M3, V1, V2, V3, A1, A2, F1, F2, F3
SVM	M1, M2, M3, V1, V2, A1, A3, F1, F2, F3
	M1, M2, M3, V1, V2, A1, A2, F1, F2, F3
	M1,M2,F2

ANN= artificial neural network; LDA= linear discriminant analysis; SVM= support vector machine; RBF= radial basis function.

V. DISCUSSION

In this paper, we proposed an innovative RDP method for the recognition of four different sleep postures with an

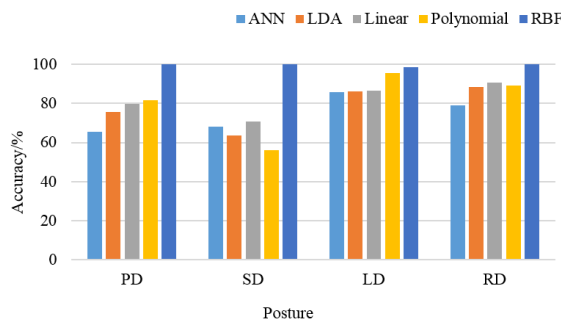


FIGURE 5. The performance of the classifier after the BE algorithm. Different posture's classification accuracy is shown in the figure, and the total accuracy of the classifiers were listed in the figure.

PRED \ GT	PD	SD	LD	RD
PD	384	0	0	0
SD	0	384	5	0
LD	0	0	379	0
RD	0	0	0	384

FIGURE 6. The confusion matrix of the SVM classifier. PRED: Predicted labels; GT: Ground-Truth; PD, SD, LD, RD corresponding to the four postures.

accuracy of 99.67%. The features extracted from dual-channel (left and right lung) bio-impedance provided high discrimination on the sleep posture recognition.

A. ASSESSMENT

Due to the difference in data and sensor, a direct comparison between our work and others is not suitable. Table 6 concluded the related studies in the familiar sleep posture recognition. The direct measure method had been studied in previous work. Heenam et al. used the patch-type device to obtain the accelerometer signal and used a DT algorithm to recognize the sleep posture and obtained an accuracy of 99.16% [30]. Xu et al. used a pressure sensor [3] to recognize the sleep posture, and achieved an accuracy of 91.21%. As a contrast, Shen et al. proposed a body position detection method by fusing multiple heterogeneous features from three-lead surface ECG, and achieved the accuracy of 66.67%. Lee et al. used unconstrained morphology of the QRS wave of ECG signals by 12 capacitively coupled electrodes and a conductive textile sheet to estimate body postures, and obtained the accuracy of 98.4% with 10-fold cross validation and SVM classifier, both of them were indirect measure methods.

In this work we proposed a novel sleep posture recognition method by measuring left and right lung respiratory impedance and obtained an accuracy of 99.67% with

BE algorithm and SVM classifier. Our work didn't rely on the sensors and the acquired 2-lead signals is relatively simple. Therefore, in the ubiquitous monitoring environment, our work may have unique advantages. Additionally, traditional single-channel impedance measuring methods [32]–[34] didn't take the influence of posture changes on sleep pulmonary volume measurement into consideration, hence we proposed a BIOPAC-based dual-channel system as a solution in our previous work [14]. However, the BIOPAC-based dual-channel system need two completely independent measurement modules (EBI100C) [14]. As a contrast, we designed a multi-channel adapter (Fig.1-(c)) to achieve single module measurement, which is lost cost and easily portable.

B. RDP BASED SLEEP POSTURE RECOGNITION ANALYSIS

Our proposed RDP based sleep posture recognition method had been introduced. This work used the BE algorithm to select the highest contribution feature, previous studies had indicated that feature selection can remove the irrelevant or redundant features therefore it was important in the pattern recognition [21]. When using all the features, the input may include much redundant information, which affects the classification accuracy, especially in the OVO-SVMs classifier using the RBF kernel. Other classifiers also had a slightly improvement after using BE algorithm. Therefore, we conclude that the BE algorithm can help improved the sleep posture recognition accuracy.

Selecting a best classifier for a particular question is important. Hence, we used 3 classical classifiers – SVM, LDA and ANN which were widely used for different pattern recognition problems, including the other relative work [12], [13]. The performance comparison is shown in Table 4, the OVO-SVMs classifier revealed excellent posture identification with a total accuracy of 99.67%. Only in the LD posture detection, our proposed algorithm miss-classified 5 samples as SD. The feature dataset selected by BE algorithm is consisted of 3 features: M1, M2, F2. Maybe the 5 samples are singular value that is similar with SD sample. Moreover, the OVO-SVMs recognition accuracy has been significantly improved while using the RBF kernel, this may be the result of the property of the RBF function. By mapping the low dimension data to the infinite dimension, the separability of the data can significantly increase [23], [28]. Moreover, SVM is an eager learning algorithm, after being trained by the training sample, it can determine a hyperplane to classify the data category. After putting the test sample into the hyperspace, its class can be determined. In previous study different multi-class SVMs were compared [29], considering the potential biases of the OVR-SVMs, we employed the OVO-SVMs in our model. The result demonstrated the ability of the OVO-SVMs classifier had high discrimination on the sleep postures recognition accuracy.

C. LIMITATIONS

Our experiment was conducted in laboratory environment with a specific sample exhibiting a very good accuracy.

TABLE 6. Comparison with related works.

Authors	Posture Recognition		Subject size	Number of sensor	Kinds of posture	Classifier	Accuracy	Highlight
	Method	Type						
Heenam et al. [30]	accelerometer sensor	Direct	13	2	5	DT	99.16%	Using accelerometer device for posture detection with high accuracy
Xu et al. [31]	pressure sensor		14	8192	6	SBSP	91.21%	Proposing BEMD approach for posture detection with high accuracy
Shen et al. [12]	EDP	In-direct	60	5	3	BPNN	66.67%	The heart axis is more accurate than HRV and PR intervals for posture detection
Lee et al. [13]	EDP		13	12	4	SVM	98.40%	Using unconstrained measurements of electrocardiogram (ECG) signals
Our work	RDP		16	6	4	SVM	99.67%	Creatively proposed a new sleep posture recognition method by measuring left and right lung respiratory impedance

EDP: electrocardiogram-derived posture; RDP: respiration-derived posture; DT: decision tree; SBSP: skew-based sleep posture (Combining kNN classifier and skew rate classifier); BEMD: body-earth mover's distance; BPNN: Back-propagation neural network; SVM: support vector machines; OVO-SVMs: One-Versus-One support vector machines.

The application of our method still needing more validation in real life because the sleep posture may not be regular in the real sleep. Age limitation in our work also needs to be considered. Besides, although our paper is based on a licensed device, design of a simpler and more integrated wearable system is desirable. Furthermore, the sample size of our experiment is relatively small. Therefore, mass and diverse samples and all-night monitoring experiment based on wearable system [35] for further verification should be contained in future studies, so that the big data analysis methods can be applied [36].

VI. CONCLUSION

In this article, we presented an innovative RDP method in identifying sleep postures for sleep quality assessment. A dual-channel respiration signal acquisition system was built based on impedance technology. The SVM classifier was applied to build a sleep posture recognition model based on backward elimination.

The following conclusions were drawn from this study:

- 1) The dual-channel respiratory and sleep posture monitoring system built in our work showed reliable ability in posture reflection (Fig.1).
- 2) We proposed a novel sleep respiration-derived posture method, which exhibited an identification accuracy of 99.67%.
- 3) We extracted 12 features for the recognition for four different sleep postures.
- 4) We modified the OVO-SVMs classifier by using backward elimination, which improved the accuracy of the model up to 99.67%. Particularly, the precision of each postures was over 98.70%.

In-situ experiment indicated that the proposed system and method were capable of offering accurate sleep posture monitoring. Furthermore, we demonstrated that our method was resilient to recognize different sleep postures. In the future, we will investigate long-term posture monitoring and mass and diverse samples, to adopt big data analysis methods and build smart home and IoT applications [37], [38].

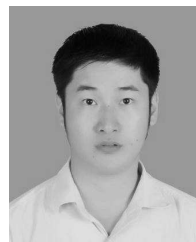
CONFLICT OF INTEREST

The authors confirm that there are no financial, personal or other conflicts of interest that could inappropriately influence this study.

REFERENCES

- [1] H. Y. Kim, H. J. Dhong, J. K. Lee, S. K. Chung, and S. C. Jung, "Sleep quality and effects of position on sleep apnea in East Asian children," *Auris Nasus Larynx*, vol. 38, no. 2, pp. 228–232, 2011.
- [2] T. V. Perneger et al., "Hospital-acquired pressure ulcers," *Arch. Internet Med.*, vol. 158, no. 17, p. 1940, 1998.
- [3] A. Oksenberg and D. S. Silverberg, "The effect of body posture on sleep-related breathing disorders: Facts and therapeutic implications," *Sleep Med. Rev.*, vol. 2, no. 3, pp. 139–162, 1998.
- [4] K. Nakajima, Y. Matsumoto, and T. Tamura, "A monitor for posture changes and respiration in bed using real time image sequence analysis," in *Proc. 22nd Annu. Int. Conf. IEEE Eng. Med. Biol. Soc.*, Jul. 2000, pp. 51–54.
- [5] M. Borazio and K. Van Laerhoven, "Combining wearable and environmental sensing into an unobtrusive tool for long-term sleep studies," in *Proc. 2nd ACM SIGKDD Symp. Int. Health Inf.-IHI*, vol. 12, Jul. 2002, pp. 71–80.
- [6] C. Wrzus, A. M. Brandmaier, T. von Oertzen, V. Müller, G. G. Wagner, and M. Riediger, "A new approach for assessing sleep duration and postures from ambulatory accelerometry," *PLoS ONE*, vol. 7, no. 10, p. e48089, 2012.
- [7] C. C. Hsia, K. J. Liou, A. P. W. Aung, V. Foo, W. Huang, and J. Biswas, "Analysis and comparison of sleeping posture classification methods using pressure sensitive bed system," in *Proc. Annu. Int. Conf. IEEE Eng. Med. Biol. Soc.*, vols. 1–20, Sep. 2009, pp. 6131–6134.

- [8] J. J. Liu et al., "Sleep posture analysis using a dense pressure sensitive bedsheet," *Pervasive Mob. Comput.*, vol. 10, pp. 34–50, Feb. 2014.
- [9] R. Yousefi et al., "Bed posture classification for pressure ulcer prevention," in *Proc. Annu. Int. Conf. IEEE Eng. Med. Biol. Soc. (EMBS)*, Aug. 2011, pp. 7175–7178.
- [10] T. Jernberg, B. Lindahl, M. Hogberg, and L. Wallentin, "Effects on QRS-waveforms and ST-T-segment by changes in body position during continuous 12-lead ECG: A preliminary report," in *Proc. Comput. Cardiol.*, vol. 24, Sep. 1997, pp. 461–464.
- [11] M. G. Adams and B. J. Drew, "Body position effects on the ECG," *J. Electrocardiol.*, vol. 30, no. 4, pp. 285–291, 1997.
- [12] T. W. Shen, F. C. Liu, Y. T. Tsao, and S. C. Chang, "A body position detection method by fusing heterogeneous information from surface ECG," in *Proc. Comput. Cardiol.*, vol. 37. Sep. 2010, pp. 517–520.
- [13] H. J. Lee et al., "Unconstrained ECG measurements," *IEEE J. Biomed. Health Inform.*, vol. 17, no. 6, pp. 985–993, Jun. 2013.
- [14] G. Liu, G. Zhou, W. Chen, and Q. Jiang, "A principal component analysis based data fusion method for estimation of respiratory volume," *IEEE Sensors J.*, vol. 15, no. 8, pp. 4355–4364, Aug. 2015.
- [15] R. Li, J. Gao, H. Wang, and Q. Jiang, "Design of a noninvasive bladder urinary volume monitoring system based on bio-impedance," *Engineering*, vol. 5, no. 10, pp. 321–325, 2013.
- [16] Q. Wang, H. Bin Wang, H. Xu, W. Zhou, and G. Z. Liu, "Noninvasive urination-desire sensing method based on bladder bioimpedance spectrum analysis," *J. Med. Biol. Eng.*, vol. 36, no. 2, pp. 191–196, 2016.
- [17] G. Liu, L. Wang, Q. Wang, G. Zhou, Y. Wang, and Q. Jiang, "A new approach to detect congestive heart failure using short-term heart rate variability measures," *PLoS ONE*, vol. 9, no. 4, p. e93399, 2014.
- [18] R. O. Duda, P. E. Hart, and D. G. Stork, *Pattern Classification*. New York, NY, USA: Wiley, 2000, p. 654.
- [19] A. K. Jain, R. P. W. Duin, and J. C. Mao, "Statistical pattern recognition: A review," *IEEE Trans. Pattern Anal. Mach. Intell.*, vol. 22, no. 1, pp. 4–37, Jan. 2000.
- [20] F. Pernkopf, "Bayesian network classifiers versus selective k-NN classifier," *Pattern Recognit.*, vol. 38, no. 1, pp. 1–10, 2005.
- [21] I. Guyon and A. Elisseeff, "An introduction to variable and feature selection," *J. Mach. Learn. Res.*, vol. 3, pp. 1157–1182, Jan. 2003.
- [22] A. Statnikov, C. F. Aliferis, and I. Tsamardinos, "Methods for multi-category cancer diagnosis from gene expression data: A comprehensive evaluation to inform decision support system development," *Stud. Health Technol. Inform.*, vol. 107, pp. 813–817, Feb. 2004.
- [23] A. Ben-Hur and J. Weston, "A user's guide to support vector machines," in *Methods in Molecular Biology*, vol. 609. 2010, pp. 223–239.
- [24] J. Shawe-Taylor and N. Cristianini, *Kernel Methods for Pattern Analysis*. Stockholm, Sweden: Vasa, 2004.
- [25] A. LanatÄ, E. P. Scilingo, E. Nardini, G. Loriga, R. Paradiso, and D. De-Rossi, "Comparative evaluation of susceptibility to motion artifact in different wearable systems for monitoring respiratory rate," *IEEE Trans. Inf. Technol. Biomed.*, vol. 14, no. 2, pp. 378–386, Mar. 2010.
- [26] T. Koivumäki, M. Vauhkonen, J. T. Kuikka, and M. A. Hakulinen, "Bioimpedance-based measurement method for simultaneous acquisition of respiratory and cardiac gating signals," *Physiol. Meas.*, vol. 33, no. 8, pp. 1323–1334, 2012.
- [27] O. Lahtinen, V. P. Seppä, J. Väistönen, and J. Hyttinen, "Optimal electrode configurations for impedance pneumography during sports activities," in *Proc. IFMBE*, vol. 22. 2008, pp. 1750–1753.
- [28] C. C. Chang and J. Lin, "A library for support vector machines," *ACM Trans. Intell. Syst. Technol.*, vol. 2, no. 3, p. 27, 2011.
- [29] C.-W. Hsu and C.-J. Lin, "A comparison of methods for multiclass support vector machines," *IEEE Trans. Neural Netw.*, vol. 13, no. 2, pp. 415–425, Mar. 2002.
- [30] H. Yoon et al., "Estimation of sleep posture using a patch-type accelerometer based device," in *Proc. Annu. Int. Conf. IEEE Eng. Med. Biol. Soc. (EMBS)*, Nov. 2015, pp. 4942–4945.
- [31] X. Xu, F. Lin, A. Wang, Y. Hu, M. C. Huang, and W. Xu, "Body-earth mover's distance: A matching-based approach for sleep posture recognition," *IEEE Trans. Biomed. Circuits Syst.*, vol. 10, no. 5, pp. 1023–1035, May 2016.
- [32] L. Poupart, M. Mathieu, R. Sartène, and M. Goldman, "Use of thoracic impedance sensors to screen for sleep-disordered breathing in patients with cardiovascular disease," *Physiol. Meas.*, vol. 29, no. 2, pp. 255–267, 2008.
- [33] Y. Yasuda, A. Umezawa, S. Horihata, K. Yamamoto, R. Miki, and S. Koike, "Modified thoracic impedance plethysmography to monitor sleep apnea syndromes," *Sleep Med.*, vol. 6, no. 3, pp. 215–224, May 2005.
- [34] V. P. SeppÄ, J. Viik, and J. Hyttinen, "Assessment of pulmonary flow using impedance pneumography," *IEEE Trans. Biomed. Eng.*, vol. 57, no. 9, pp. 2277–2285, Sep. 2010.
- [35] M. Chen, Y. Ma, Y. Li, D. Wu, Y. Zhang, and C. H. Youn, "Wearable 2.0: Enable human-cloud integration in next generation healthcare system," *IEEE Commun. Mag.*, vol. 55, no. 1, pp. 54–61, Jan. 2017.
- [36] M. Chen, Y. Hao, K. Hwang, L. Wang, and L. Wang, "Disease Prediction by Machine Learning over Big Healthcare Data," *IEEE Access*, vol. 5, no. 1, pp. 8869–8879, 2017.
- [37] M. Chen, P. Zhou, and G. Fortino, "Emotion communication system," *IEEE Access*, vol. 5, pp. 326–337, 2017.
- [38] M. Chen, J. Yang, X. Zhu, X. Wang, M. Liu, and J. Song, "Smart home 2.0: Innovative smart home system powered by botanical IoT and emotion detection," *Mobile Netw. Appl.*, vol. 6, no. 3, pp. 1–11, Apr. 2017, doi: 10.1007/s11036-017-0866-1.



GUANZHENG LIU received the degree from the University of the Chinese Academy of Sciences in 2011. Since 2012, he has been with the School of Engineering, Sun Yat-sen University, as a Lecturer. His research interests include biomedical signal processing, body sensor networks, and pattern recognition.



KUNYANG LI received the degree from the Guilin University of Electronic Technology, Guilin, China, in 2014. He is currently pursuing the master's degree with the School of Engineering, Sun Yat-sen University, Guangzhou, China.

His research interests include biomedical signal processing and pattern recognition.



LIANRONG ZHENG received the bachelor's degree in biomedical engineering from Tianjin Medical University, Tianjin, China. She is currently pursuing the master's degree in biomedical engineering with Sun Yat-sen University, Guangzhou, China. Her research interest is biomedical signal processing.



WEN-HUI CHEN received the bachelor's degree in biomedical engineering from Beijing Jiaotong University, Beijing, China. She is currently pursuing the master's degree in biomedical engineering with Sun Yat-sen University, Guangzhou, China. Her research interests include biomedical signal processing.



GUANGMIN ZHOU received the bachelor's degree from Xinxiang Medical University, Xinxiang, China, in 2013. She is currently pursuing the master's degree in biomedical engineering with Sun Yat-sen University, Guangzhou, China.

Her research interest is biomedical signal processing.



QING JIANG received the Ph.D. degree in engineering and applied science from the California Institute of Technology, USA, in 1990. He is currently a Professor with the School of Engineering, Sun Yat-sen University, Guangzhou, China.

His research interests include smart materials and smart structures, intelligent microelectromechanical systems and devices, nanotechnology and electromechanical device system, and medical engineering.

• • •